13 Avital S, Zundel N, Szomstein S, Rosenthal R. Laparoscopic transhiatal esophagectomy for esophageal cancer. Am J Surg 2005; 190: 69–74.
14 Dapri G, Himpens J, Cadiere G B. Minimally invasive esophagectomy for cancer: laparoscopic transhiatal procedure or thoracoscopy in prone position followed by laparoscopy? Surg Endosc 2008; 22: 1060–69.
15 Scheepers J J, Veenhof A A, van der Peet D L *et al.* Laparoscopic transhiatal resection for malignancies of the distal esophagus: outcome of the first 50 resected patients. Surgery 2008; 143: 278–85.
16 Montenovo M I, Chambers K, Pellegrini C A, Oelschlager B K. Outcomes of laparoscopic-assisted transhiatal esophagectomy for adenocarcinoma of the esophagus and esophago-gastric junction. Dis Esophagus 2011; 24: 430–36.
17 Van den Broek W T, Makay O, Berends F J *et al.* Laparoscopically assisted transhiatal resection for malignancies of the distal esophagus. Surg Endosc 2004; 18: 812–7.
18 Bernabe K Q, Bolton J S, Richardson W S. Laparoscopic hand-assisted versus open transhiatal esophagectomy: a case–control study. Surg Endosc 2005; 19: 334–7.
19 Shiozaki A, Fujiwara H, Murayama Y *et al.* Posterior mediastinal lymph node dissection using the pneumomediastinum method for esophageal cancer. Esophagus 2011; 9: 58–64.
20 Shiozaki A, Fujiwara H, Murayama Y *et al.* Perioperative outcomes of esophagectomy preceded by the laparoscopic transhiatal approach for esophageal cancer. Dis Esophagus 2012; 27: 470–78.
21 Udagawa H, Ueno M, Shinohara H *et al.* The importance of grouping of lymph node stations and rationale of three-field lymphoadenectomy for thoracic esophageal cancer. J Surg Oncol 2012; 106: 742–7.
22 Sobin L H, Gospodarowicz M K, Wittekind C. TNM Classification of Malignant Tumours (UICC International Union Against Cancer), 7th edn. Oxford: Wiley-Blackwell, 2009.
23 Japan Esophageal Society. Japanese Classification of Esophageal Cancer, 10th edn. Tokyo: Kanehara & Co, 2008.
24 American Society of Anesthesiologists. New classification of physical status. Anesthesiology 1963; 24: 111.
25 Dindo D, Demartines N, Clavien P A. Classification of surgical complications: a new proposal with evaluation in a cohort of 6336 patients and results of a survey. Ann Surg 2004; 240: 205–13.
26 Shiozaki A, Fujiwara H, Konishi H *et al.* Novel technique for dissection of subcarinal and main bronchial lymph nodes using a laparoscopic transhiatal approach for esophageal cancer. Anticancer Res 2013; 33: 2577–85.
27 Peyre C G, Hagen J A, DeMeester S R *et al.* The number of lymph nodes removed predicts survival in esophageal cancer: an international study on the impact of extent of surgical resection. Ann Surg 2008; 248: 549–56.
28 Altorki N K, Zhou X K, Stiles B *et al.* Total number of resected lymph nodes predicts survival in esophageal cancer. Ann Surg 2008; 248: 221–6.
29 Greenstein A J, Litle V R, Swanson S J, Divino C M, Packer S, Wisnivesky J P. Effect of the number of lymph nodes sampled on postoperative survival of lymph node-negative esophageal cancer. Cancer 2008; 112: 1239–46.
30 Noshiro H, Iwasaki H, Kobayashi K *et al.* Lymphadenectomy along the left recurrent laryngeal nerve by a minimally invasive esophagectomy in the prone position for thoracic esophageal cancer. Surg Endosc 2010; 24: 2965–73.
31 Ozawa S, Ito E, Kazuno A *et al.* Thoracoscopic esophagectomy while in a prone position for esophageal cancer: a preceding anterior approach method. Surg Endosc 2013; 27: 40–47.
32 Watanabe M, Baba Y, Nagai Y, Baba H. Minimally invasive esophagectomy for esophageal cancer: an updated review. Surg Today 2013; 43: 237–44.
33 Orringer M B, Marshall B, Chang A C *et al.* Two thousand transhiatal esophagectomies: changing trends. Ann Surg 2007; 246: 363–72, discussion 372–4.
34 Gockel I, Kneist W, Keilmann A, Junginger T. Recurrent laryngeal nerve paralysis (RLNP) following esophagectomy for carcinoma. Eur J Surg Oncol 2005; 31: 277–81.
35 Hulscher J B, van Sandick J W, Devriese P P, van Lanschot J J, Obertop H. Vocal cord paralysis after subtotal oesophagectomy. Br J Surg 1999; 86: 1583–7.

# *xCT, component of cysteine/glutamate transporter, as an independent prognostic factor in human esophageal squamous cell carcinoma*

**Atsushi Shiozaki, Daisuke Iitaka, Daisuke Ichikawa, Shingo Nakashima, Hitoshi Fujiwara, Kazuma Okamoto, Takeshi Kubota, et al.**

**Journal of Gastroenterology**

ISSN 0944-1174
Volume 49
Number 5

J Gastroenterol (2014) 49:853-863
DOI 10.1007/s00535-013-0847-5

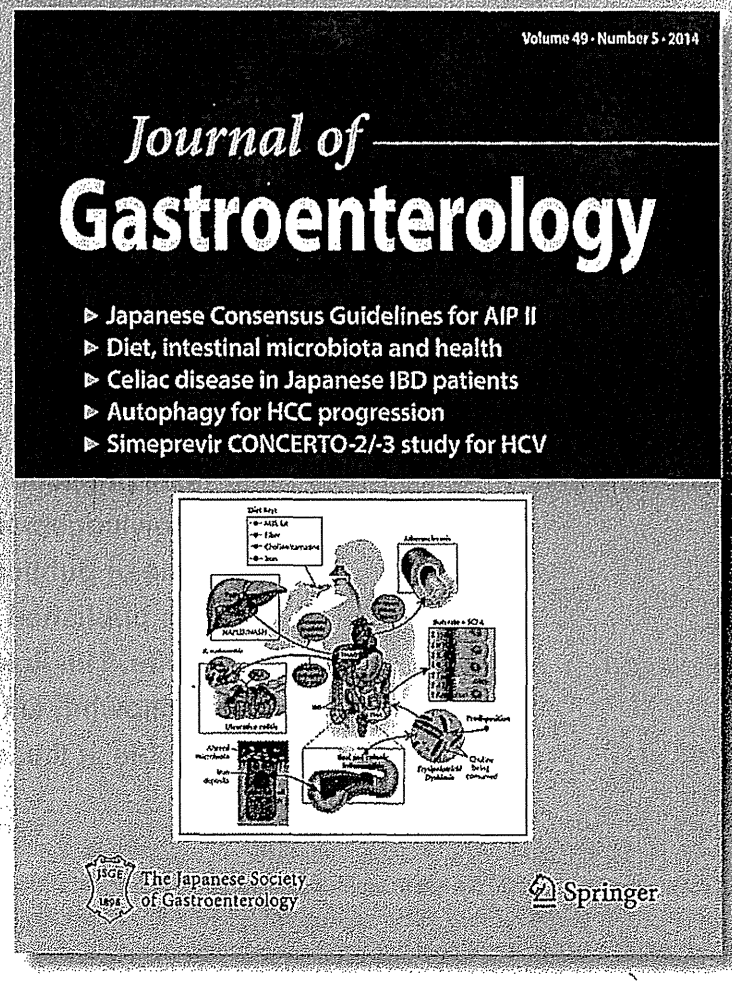


Springer

J Gastroenterol (2014) 49:853–863
DOI 10.1007/s00535-013-0847-5

The Japanese Society of Gastroenterology

ORIGINAL ARTICLE—ALIMENTARY TRACT

# xCT, component of cysteine/glutamate transporter, as an independent prognostic factor in human esophageal squamous cell carcinoma

Atsushi Shiozaki · Daisuke Iitaka · Daisuke Ichikawa · Shingo Nakashima · Hitoshi Fujiwara · Kazuma Okamoto · Takeshi Kubota · Shuhei Komatsu · Toshiyuki Kosuga · Hiroki Takeshita · Hiroki Shimizu · Yoshito Nako · Hisami Sasagawa · Mitsuo Kishimoto · Eigo Otsuji

Received: 25 September 2012 / Accepted: 31 May 2013 / Published online: 17 June 2013


**Abstract**
*Background* xCT is a component of the cysteine/glutamate transporter, which plays a key role in glutathione synthesis. The objectives of the present study were to investigate the role of xCT in the regulation of genes involved in cell cycle progression and the clinicopathological significance of its expression in esophageal squamous cell carcinoma (ESCC).
*Methods* xCT expression in human ESCC cell lines was analyzed by Western blotting and immunofluorescent staining. Knockdown experiments were conducted with xCT siRNA, and the effect on cell cycle was analyzed. The cells' gene expression profiles were analyzed by microarray analysis. An immunohistochemical analysis of 70 primary tumor samples obtained from ESCC patients that had undergone esophagectomy was performed.
*Results* xCT was highly expressed in TE13 and KYSE170 cells. In these cells, the knockdown of xCT using siRNA inhibited $G_1$-S phase progression. Microarray analysis identified 1652 genes whose expression levels in TE13 cells were altered by the knockdown of xCT. Pathway analysis showed that the top-ranked canonical pathway was the $G_1$/S checkpoint regulation pathway, which involves TP53INP1, CDKN1A, CyclinD1/cdk4, and E2F5. Immunohistochemical staining showed that xCT is mainly found in the nuclei of carcinoma cells, and that its expression is an independent prognostic factor.
*Conclusions* These observations suggest that the expression of xCT in ESCC cells might affect the $G_1$/S checkpoint and impact on the prognosis of ESCC patients. As a result, we have a deeper understanding of the role played by xCT as a mediator and/or biomarker in ESCC.

**Keywords** xCT/SLC7A11 · Esophageal cancer · Cell cycle

A. Shiozaki and D. Iitaka contributed equally to this work.

**Electronic supplementary material** The online version of this article (doi:10.1007/s00535-013-0847-5) contains supplementary material, which is available to authorized users.

A. Shiozaki (✉) · D. Iitaka · D. Ichikawa · S. Nakashima · H. Fujiwara · K. Okamoto · T. Kubota · S. Komatsu · T. Kosuga · H. Takeshita · H. Shimizu · Y. Nako · E. Otsuji
Division of Digestive Surgery, Department of Surgery, Kyoto Prefectural University of Medicine, 465 Kajii-cho, Kamigyo-ku, Kyoto 602-8566, Japan
e-mail: shiozaki@koto.kpu-m.ac.jp

H. Sasagawa
School of Nursing, Kyoto Prefectural University of Medicine, Kyoto 602-8566, Japan

M. Kishimoto
Department of Pathology, Kyoto Prefectural University of Medicine, Kyoto 602-8566, Japan

## Introduction

xCT, or SLC7A11 (solute carrier family 7, membrane 11), encodes the transporter subunit of the $Na^+$-independent heterodimeric amino acid transport system xc- [1, 2]. System xc-, which consists of xCT and a regulatory heavy chain component (4F2hc), functions as an exchange system for cystine/glutamate with cystine entering cells in exchange for the release of glutamate in a 1:1 ratio. xCT expression at the cell surface is essential for the uptake of cysteine, which is required for intracellular glutathione (GSH) synthesis and, thus, is an important determinant of the intracellular redox balance [3, 4].

In human cancer cells, cystine uptake is largely mediated by system xc-, and high expression levels of xCT have

been demonstrated in a variety of human carcinomas, including glioma and colon, breast, prostate, ovarian, pancreatic, gastric, and esophageal cancer [5–12]. There are several reports about the role of xCT in cancer cell proliferation. Lyons et al. [13] showed that xCT affects glioma invasion through the autocrine glutamate signaling loop in the brain. Ishimoto et al. [11] showed that CD44 variants regulate redox status in gastrointestinal cancer cells by stabilizing the xCT subunit, and thus, promote tumor growth. Furthermore, Chen et al. [12] showed that disruption of xCT inhibits esophageal cancer cell metastasis via the caveolin-1/b-catenin pathway. Although these studies suggest that the modulation of xCT activity is an intriguing strategy for cancer therapy, the detailed mechanisms by which xCT regulates the proliferation of esophageal squamous cell carcinoma (ESCC) cells have not been fully investigated. Furthermore, the clinicopathological impact of xCT expression in ESCC remains uncertain.

The objectives of the present study were to investigate the role of xCT in the regulation of genes involved in cell cycle progression and the clinicopathological significance of its expression in ESCC. Our results indicate that xCT plays an important role in the tumor progression of ESCC.

## Materials and methods

### Cell lines, antibodies, and other reagents

The poorly differentiated human ESCC cell lines TE2, TE5, TE9, and TE13 were obtained from the Cell Resource Center for Biomedical Research Institute of Development, Aging, and Cancer (Tohoku University, Sendai, Japan) [14]. The human ESCC cell lines KYSE70 and KYSE170 were obtained from Kyoto University (Kyoto, Japan) [15]. These cells were grown in RPMI-1640 medium (Nacalai Tesque, Kyoto, Japan) supplemented with 100 U/ml of penicillin, 100 μg/ml of streptomycin, and 10 % fetal bovine serum (FBS). The cells were cultured in flasks and dishes in a humidified incubator at 37 °C under 5.0 % $CO_2$ in air.

The anti-xCT antibody used for the immunofluorescent and immunohistochemical analysis came from Trans Genic Inc. (Kumamoto, Japan), and that for the protein assay came from Novus Biologicals (Littleton, CO, USA). Anti-Ki67 antibody was obtained from Santa Cruz Biotechnology (Santa Cruz, CA, USA). Antibodies for p21, horseradish peroxidase (HRP)-conjugated horse anti-mouse and goat anti-rabbit secondary antibodies were purchased from Cell Signaling Technology (Beverly, MA, USA), and the antibody for glyceraldehyde-3-phosphate dehydrogenase (GAPDH) was from Santa Cruz Biotechnology. A monoclonal cyclin D1 (CCND1) antibody was from Abcam (clone SP4, Cambridge, MA, UK). The Alexa Fluor 488 labeled goat anti-rabbit secondary antibody was from Invitrogen (Carlbad, CA, USA), and the rhodamine phalloidin was from Cytoskeleton (Denver, CO, USA).

### Western blotting

The cells were harvested in M-PER lysis buffer (Pierce, Rockford, IL, USA) supplemented with protease inhibitors (Pierce, Rockford, IL, USA). The protein concentration was measured with a modified Bradford assay (Bio-Rad, Hercules, CA, USA). Cell lysates containing equal amounts of total protein were separated by SDS-PAGE and then transferred onto PVDF membranes (GE Healthcare, Piscataway, NJ, USA). The membranes were then probed with the indicated antibodies, and proteins were detected by an ECL Plus Western Blotting Detection System (GE Healthcare, Piscataway, NJ, USA). Separation and preparation of cytoplasmic and nuclear extracts from ESCC cell lines were performed according to the manufacturer's instructions by using the NE-PER Nuclear and Cytoplasmic Extraction Reagents (Thermo Scientific, Rockford, IL, USA).

### Immunofluorescent staining and confocal microscopy

ESCC cells were cultured on glass coverslips for 72 h. Thereafter, the cells were fixed with 4 % paraformaldehyde for 20 min at room temperature and permeabilized in 0.25 % Triton X-100 in phosphate-buffered saline. The cells were then incubated with anti-xCT antibody for 2 h at room temperature. After being washed three times in PBS, the cells were incubated with Alexa Fluor 488 labeled goat anti-rabbit secondary antibodies and rhodamine phalloidin for 1 h at room temperature. Slides were then mounted with VECTASHIELD mounting medium and 4′,6-diamidino-2-phenylindole (DAPI) (Vector Laboratories, Burlingame, CA, USA), and the distribution of xCT was examined by confocal fluorescence microscopy (LSM510; Carl Zeiss Co. Ltd, Germany).

### Small interference RNA (siRNA) transfection

Loss-of-function screening was performed using siRNA targeting xCT mRNA (Santa Cruz Biotechnology). The cells were transfected with 50 nM xCT siRNA using Lipofectamine 2000 (Invitrogen, St Louis, MO, USA) according to the manufacturer's instructions. The medium containing siRNA was replaced with fresh medium after 24 h. Control siRNA from Santa Cruz Biotechnology was used as a negative control.

### Cell cycle analysis

The cell cycle was evaluated at 48 h after the siRNA transfection by fluorescence-activated cell scoring (FACS). Briefly, the cells were treated with Triton X-100 and RNase, and their nuclei were stained with propidium iodide (PI) before their DNA content was measured using a Becton–Dickinson FACS Calibur (Becton–Dickinson, Mountain view, CA, USA). At least 10,000 cells were counted, and the ModFit LT software (Verity Software House, Topsham, ME, USA) was used to analyze cell cycle distribution.

### Cell proliferation

Cells were seeded onto 6-well plates at a density of $1.0 \times 10^5$ cells per well and incubated at 37 °C with 5 % $CO_2$. At 24 h after the cell seeding, the siRNA transfection was performed. At 48 h after the siRNA transfection, the cells were detached from the flasks in trypsin–EDTA solution and counted with a hemocytometer.

### Patients and primary tissue samples

ESCC tumor samples were obtained from 70 patients with histologically-proven primary ESCC who underwent esophagectomy (potentially curative R0 resection) at Kyoto Prefectural University of Medicine (Kyoto, Japan) between 1998 and 2007 and embedded in paraffin after 12 h formalin fixation. The patient eligibility criteria were as follows: no synchronous or metachronous cancers (in addition to the ESCC) and no preoperative chemotherapy or radiation therapy. We excluded the patients with non-curative resected tumor or non-consecutive data. All patients gave written informed consent. Relevant clinicopathological and survival data were obtained from the hospital database. Twenty-two patients (31.4 %) died of cancer recurrence. Staging was principally based on the International Union Against Cancer (UICC)/TNM Classification of Malignant Tumors (7th edition) [16].

### Immunohistochemistry

Paraffin sections (4 μm thick) of the tumor tissues were subjected to immunohistochemical staining for the xCT protein using the avidin–biotin-peroxidase method. Briefly, paraffin sections were dewaxed in xylene and dehydrated through a graded series of alcohols. Antigen retrieval was performed by heating the samples in Dako REAL Target Retrieval Solution (Glostrup, Denmark) for 40 min at 98 °C. Endogenous peroxidases were quenched by incubating the sections for 30 min in 0.3 % $H_2O_2$. The sections were then treated with protein blocker and incubated overnight at 4 °C with anti-xCT or anti-Ki67 antibody. The avidin–biotin-peroxidase complex system (Vectastain ABC Elite kit; Vector laboratories, Burlingame, CA, USA) was used for color development with diaminobenzidine tetrahydrochloride. The sections were counterstained with hematoxylin. Finally, the sections were dehydrated through a graded series of alcohols, cleared in xylene, and mounted.

Tumor cells with nuclei containing brown immunoreactive products were considered to be positive for xCT, Ki-67, p21 or CCND1 expression. Control sections of known cases of ESCC were included in each run, and negative control sections were produced by omitting the primary antibody. To evaluate the positivity rate, the numbers of xCT, Ki-67, p21 or CCND1 stained cells were quantified in five randomly selected fields at a magnification of 400×. The positivity rate in each case was calculated as the number of positive cells divided by the total number of examined cells in all examined fields.

### Real time reverse transcription-polymerase chain reaction (RT-PCR)

Total RNA was isolated from the ESCC cell lines using an RNeasy Mini kit (Qiagen, MD, USA). The primers used for the quantitative RT-PCR are shown in Supplementary Table 1. Quantitative real-time one-step RT-PCR was performed by monitoring the increase in the fluorescence of SYBER GREEN I dye with a QuantiTect SYBR Green RT-PCR kit (Qiagen, Hilden, Germany) and the Light Cycler 1.5 instrument (Roche Diagnostics, Basel, Switzerland) according to the manufacturer's protocol. All assays were performed in triplicate. Gene expression levels were normalized to the level of β2MG.

### Microarray sample preparation and hybridization

RNA integrity was determined using an Agilent 2100 Bioanalyzer (Agilent Technologies Inc., Santa Clara, CA, USA). We followed the standard Affymetrix protocols to perform the gene expression profiling experiments using Human Gene 1.0 ST arrays (Affymetrix, Santa Clara, CA, USA). Two hundred and fifty ng of total RNA were amplified and labeled with the Ambion® WT Expression Kit (Ambion, Austin, TX) and GeneChip® WT Terminal Labeling kit (Affymetrix). Array hybridization was carried out on a GeneChip® platform (Affymetrix). The labeled cDNA was hybridized to Human Gene 1.0 ST arrays for 17 h, and then washed, stained with streptavidin–phycoerythrin, and scanned.

### Processing of microarray data

Data analysis was performed using the Affymetrix Expression Console software (Affymetrix). Raw data were

normalized with RMA-sketch using the default settings of the Expression Console for Gene 1.0 ST arrays. Signal transduction networks were analyzed by Ingenuity Pathway Analysis (IPA) (Ingenuity Systems, Inc., Redwood City, CA, USA).

### Statistical analysis

The chi-square test or Fisher's exact test was used to evaluate differences between proportions, and Student's *t* test was used to evaluate continuous variables. Survival curves were constructed by the Kaplan–Meier method, and differences in survival were examined using the log-rank test. A multivariate analysis of factors influencing survival was performed using the Cox proportional hazards model. Differences were considered significant when the relevant *p* value was $<0.05$.

These analyses were performed using statistical software (JMP, version 8, SAS Institute Inc., Cary, NC, USA). Correlation analysis was performed by creating Fit Y by X plots using JMP.

## Results

### Expression of xCT in ESCC cells

To determine the role of xCT in ESCC, we first examined six ESCC cell lines, TE2, TE5, TE9 TE13, KYSE70, and KYSE170, for xCT protein expression. Western blotting revealed that xCT was expressed in all 6 cell lines, and higher levels of expression were observed in the TE13 and KYSE170 cell lines (Fig. 1a). The subcellular distribution of xCT protein in TE13 and KYSE170 cells was determined with confocal microscopy. Immunofluorescent staining with xCT antibody demonstrated that xCT was predominantly distributed in the nucleus of TE13 and KYSE170 cells (Fig. 1b). Further, cytoplasmic and nuclear extracts were separated from TE13 or KYSE170 cell lines, and we found xCT expressions in nuclear extracts of both cell lines (Supplementary Fig. 1).

### xCT controls the cell cycle progression of ESCC cells

We conducted knockdown experiments with xCT siRNA in TE13 and KYSE170 cells, and analyzed the effects of xCT knockdown on cell cycle progression. xCT siRNA effectively reduced the xCT protein levels (Fig. 2a) and xCT mRNA levels (Fig. 2b) of the TE13 and KYSE170 cell lines. The downregulation of xCT partially reduced cell cycle progression from the $G_1$ to S phase (Fig. 2c). At 48 h after the siRNA transfection, the cell counts of the xCT siRNA transfected cells were significantly lower than those of the control siRNA transfected cells (Fig. 2d). These results suggest that xCT plays an important role in the regulation of cell cycle progression and cell proliferation in ESCC cells.

### Gene expression profile of xCT siRNA transfected cells

To determine the molecular mechanisms by which xCT regulates cellular functions, we analyzed the gene expression profiles of xCT siRNA transfected TE13 cells in microarray and bioinformatics studies. Microarray analysis showed that the expression levels of 1652 genes displayed fold changes of $>1.5$ in TE13 cells subjected to xCT knockdown. Of the genes, 931 were upregulated, and 721 were downregulated in the xCT siRNA transfected TE13 cells. The 50 genes whose expression levels were most strongly up- or downregulated in the xCT siRNA transfected TE13 cells are shown in Supplementary Table 2. xCT expression was downregulated in the xCT siRNA transfected TE13 cells (fold change: −2.5; Supplementary Table 2). Ingenuity Pathway Analysis showed that cancer was one of the top-ranked diseases related to xCT (Supplementary Table 3). Furthermore, "Cell Cycle: G1/S Checkpoint Regulation" was one of the top-ranked canonical pathways related to xCT (Supplementary Table 3). Among the 1652 genes whose expression levels were changed by xCT knockdown, 248 genes had cell proliferation-related functions (cellular growth and proliferation, cell cycle, cell death, or cellular development) (data not shown). Among these genes, 105 genes were upregulated, and the other 143 genes were downregulated (data not shown). We then examined the signal transduction networks induced by the knockdown of xCT expression (Supplementary Table 3). One of the top-ranked signal networks was "Cell Cycle, Amino Acid Metabolism, Small Molecular Biochemistry", which includes TP53INP1, CDKN1A (p21), cyclin D1/cdk4, and E2F5 (Supplementary Fig. 2). These results indicate that the expression level of xCT influences genes related to cellular growth and cell cycle progression.

### Verification of gene expression by real-time quantitative RT-PCR

Four genes (cyclin D1, E2F5, p21, and TP53INP1) were examined further using quantitative RT-PCR. The expression levels of cyclin D1, E2F5, p21, and TP53INP1 mRNA were significantly decreased in the xCT siRNA transfected TE13 cells compared with the control siRNA transfected cells (Fig. 3). Furthermore, the expression levels of these 4 genes were also significantly decreased in the xCT siRNA transfected KYSE170 cells compared with the control siRNA transfected cells (Fig. 3). These changes are in agreement with the microarray results.

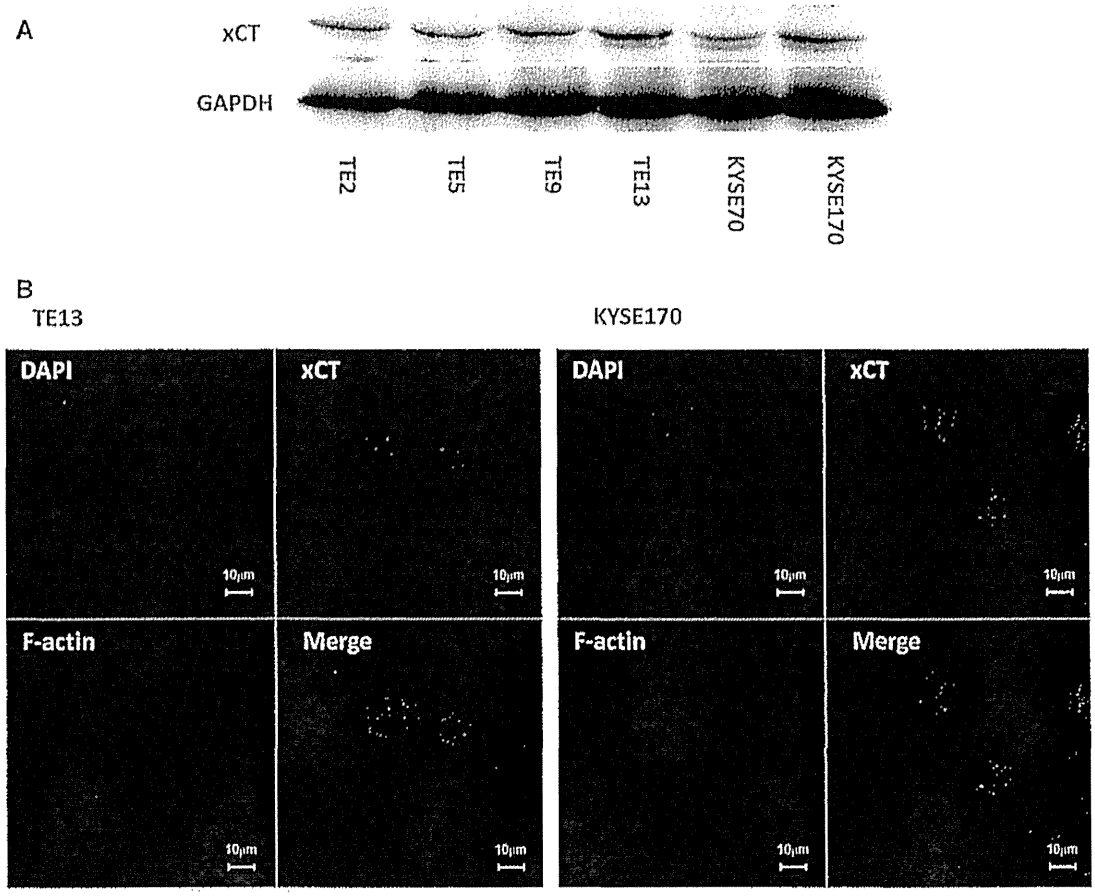


Fig. 1 Expression of xCT in ESCC cells. a xCT protein expression was analyzed in 6 ESCC cell lines. Western blotting revealed that xCT was expressed in all 6 cell lines, and higher levels of expression were observed in the TE13 and KYSE170 cell lines. b The subcellular distribution of xCT protein was determined by confocal microscopy. Immunofluorescent staining with xCT antibody demonstrated that xCT was mainly distributed in the nucleus

xCT protein expression in human ESCC

We further examined the expression of xCT in 70 primary tumor samples of human ESCC based on their immunohistochemical reactivity. An immunohistochemical examination of non-cancerous esophageal epithelia performed with xCT antibody demonstrated that xCT expression was chiefly confined to the parabasal cell layer and that xCT-positive cells could be clearly identified by their brown nuclear staining (Fig. 4a). Figure 4b shows the typical xCT immunohistochemistry findings obtained in the ESCC patients. xCT was mainly found in the nuclei of the carcinoma cells, as was found during the immunofluorescent staining of ESCC cell lines (Fig. 4c).

Next, we analyzed the relationship between xCT and Ki-67 expression, a cell proliferation marker, by immunohistochemistry with Ki-67 antibody (Fig. 4c). Ki-67 labeling tumor cells were clearly identified by their brown nuclear staining, and the distribution of Ki-67 in ESCC was similar to the distribution of xCT (Fig. 4c). In 70 primary tumor samples, the mean xCT positivity rate was 24.7 % (range 0.6–74.8 %), and the mean Ki-67 labeling index was 28.3 % (range, 2.9–55.9 %). The xCT positivity rate was positively correlated with the Ki-67 labeling index ($R^2 = 0.117$, $p = 0.0038$) (Fig. 4d). These results suggest that xCT plays an important role in the proliferation of ESCC cells. Further, we analyzed p21 and CCND1 labeling index by immunohistochemistry. Immunohistochemistry staining revealed that the expression of p21 or CCND1were clearly identified in the nucleus of ESCC (Supplementary Fig 3AB). The xCT positivity rate was not correlated with the p21 labeling index ($p = 0.97$) (Supplementary Fig 3C). Further, the xCT positivity rate was not correlated with the CCND1 labeling index ($p = 0.28$) (Supplementary Fig 3D).

We divided the ESCC patients into 2 groups, the xCT positivity rate of <20 % ($n = 35$) and xCT positivity rate of ≥20 % ($n = 35$) groups, and compared their clinicopathological features. The median and mean xCT positivity rate of the low expression group were 10.1 and 10.5 % (range 0.6–19.7 %), respectively. The median and mean

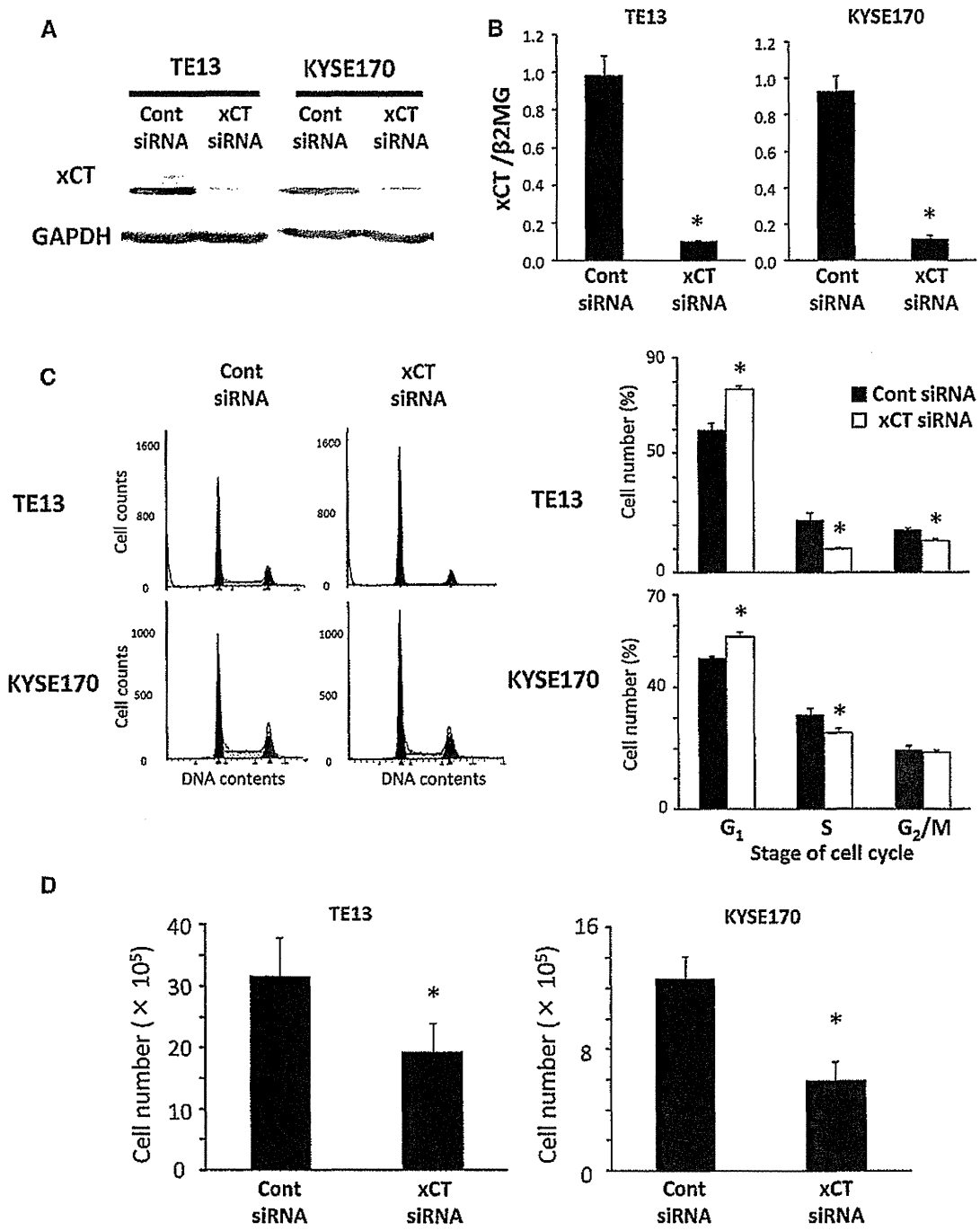


Fig. 2 xCT controls the cell cycle progression of ESCC cells. a Western blotting revealed that xCT siRNA effectively reduced the protein levels of xCT in the TE13 and KYSE170 cells. b xCT siRNA effectively reduced the mRNA levels of xCT in the TE13 and KYSE170 cells. Mean ± SEM. $n = 5$. *$p < 0.05$ (compared with the control siRNA group). c xCT downregulation partially reduced cell cycle progression from $G_1$ to S phase in the TE13 and KYSE170 cells. Cells that had been transfected with the control or xCT siRNA were stained with propidium iodide (PI) and analyzed by flow cytometry. Mean ± SEM. $n = 5$. *$p < 0.05$ (compared with control siRNA). d xCT downregulation inhibited the proliferation of the TE13 and KYSE170 cells. The number of cells was counted at 48 h after siRNA transfection. Mean ± SEM. $n = 4$. *$p < 0.05$ (compared with control siRNA)

xCT positivity rate of the high expression group were 36.6 and 38.9 % (range 20.1–74.8 %), respectively. No correlation was found between the xCT positivity rate and any other clinicopathological parameter; i.e., pT, pN, pStage, histological type, lymphatic invasion, or venous invasion (Table 1).

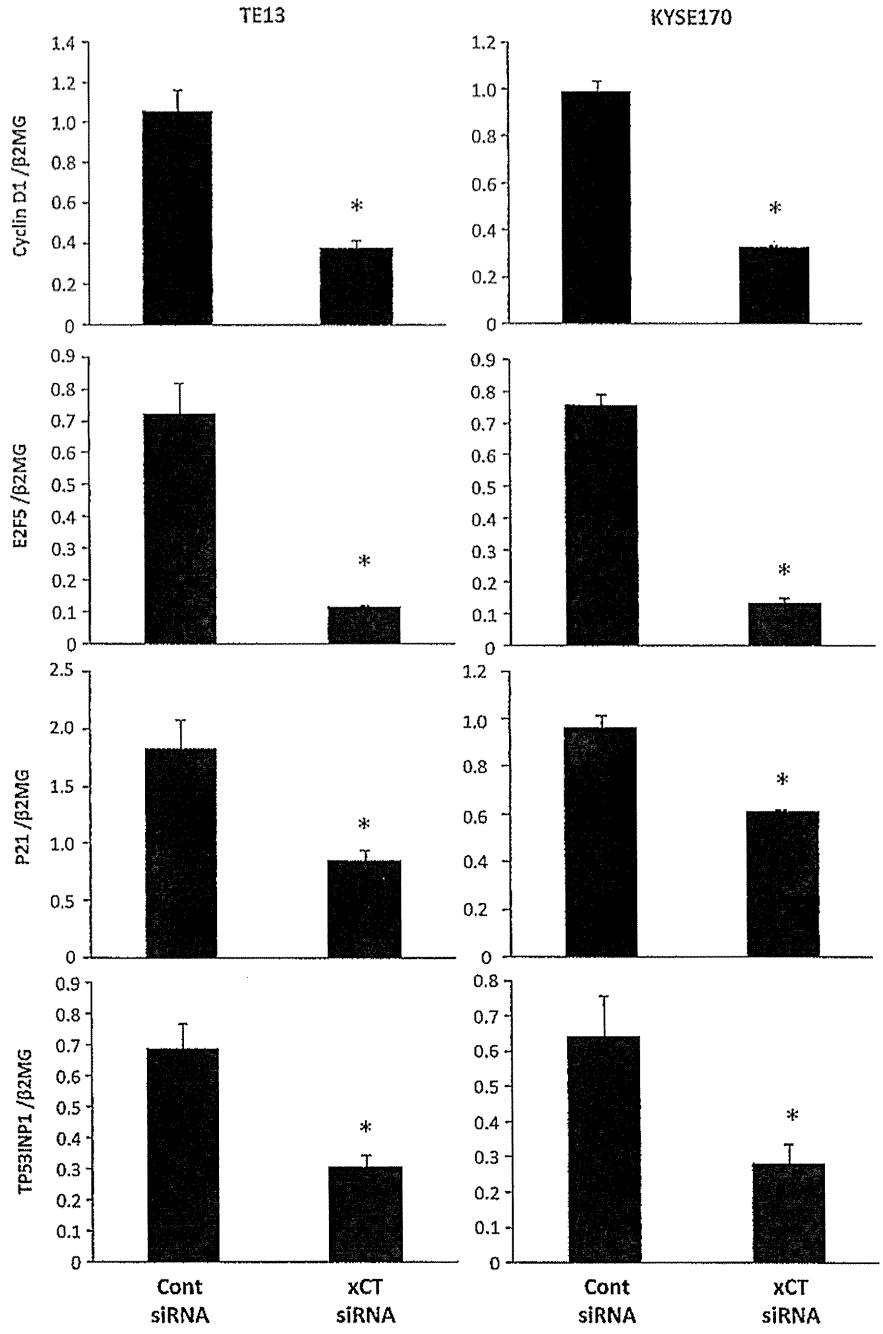


Fig. 3 Verification of gene expression by real-time quantitative RT-PCR. The expression levels of four selected genes (cyclin D1, E2F5, p21 and TP53INP1) in xCT siRNA transfected TE13 and KYSE170 cells were compared with those in the control siRNA transfected cells using real-time quantitative RT-PCR. Gene expression levels were normalized to the level of β2MG. Mean ± SEM. $n = 5$. *$p < 0.05$ (compared with control siRNA)

We also assessed which of 8 variables (pT, pN category, pStage, histological type, lymphatic invasion, venous invasion, Ki-67 labeling index and xCT positivity rate (cut off value 20 %) influence survival after the curative resection of esophageal cancer. In a univariate analysis of survival after esophagectomy, pT, pN category, pStage, lymphatic invasion and venous invasion were found to be prognostic factors ($p = 0.004$, 0.005, 0.012, 0.017, and 0.028, respectively) (Table 2). The 5-year survival rate of the patients with low xCT expression (76.2 %) was higher than that of the patients with high expression (56.8 %), although there was no statistical difference ($p = 0.056$) (Table 2) (Supplementary Fig. 4). When the patients were divided into two groups using an Ki-67 labeling index cut off value of 35 %, the 5-year survival rate of the patients with Ki-67 labeling index of ≥35 % was 74.5 %, which was significantly higher than that of the patients with Ki-67 LI of <35 % (40.7 %). Multivariable analysis demonstrated that venous invasion, Ki-67 labeling index and the xCT positivity rate were independent prognostic factors ($p = 0.010$,

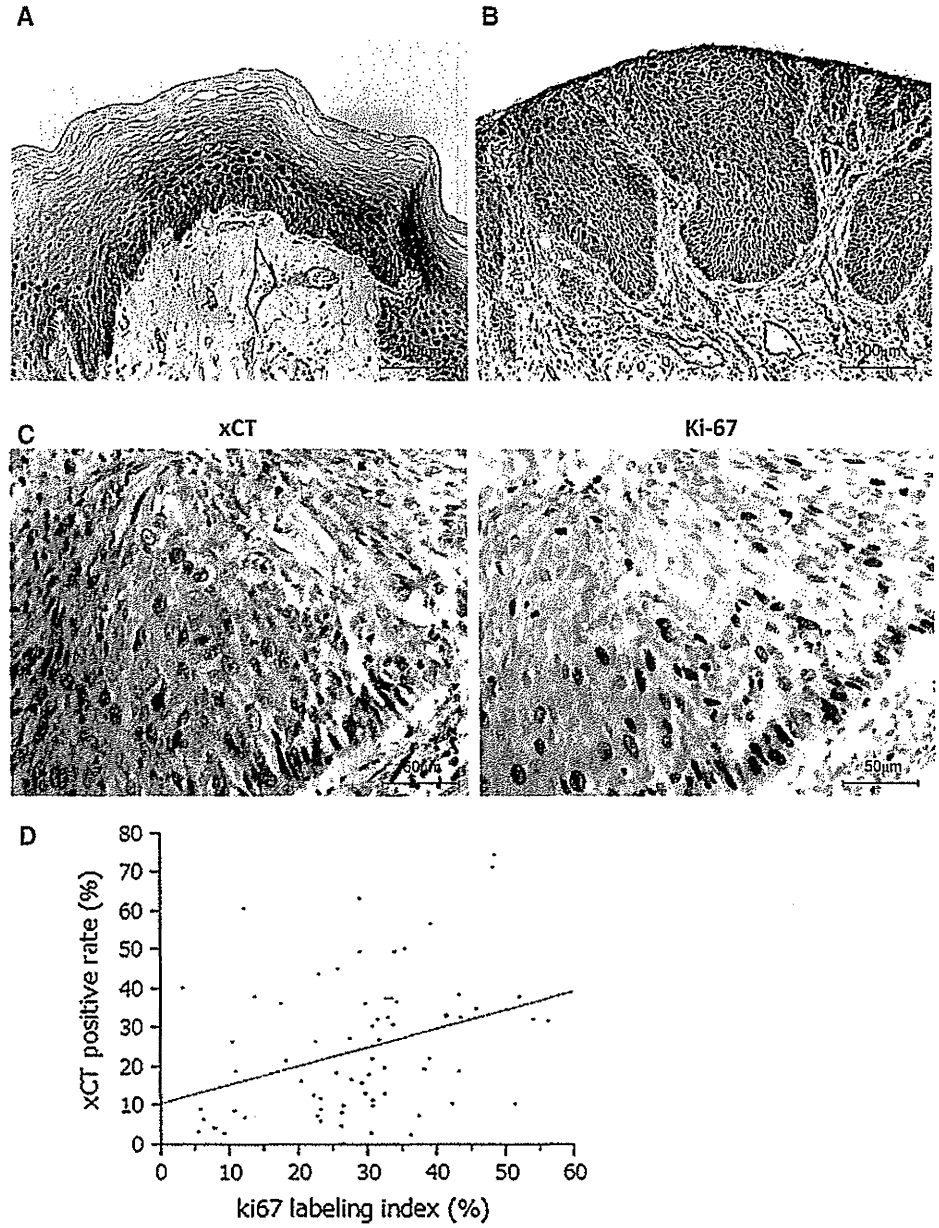


**Fig. 4** xCT protein expression in human ESCC. a Immunohistochemical staining of human esophageal epithelia with xCT antibody. xCT expression was chiefly confined to the parabasal cell layer. b Immunohistochemical staining with xCT antibody for human ESCC. Marked xCT expression was observed in ESCC. c Intracellular distribution of xCT and Ki-67 proteins in ESCC. xCT was mainly found in the nuclei of the carcinoma cells. Ki-67 labeling tumor cells were clearly identified by their brown nuclear staining, and their distribution in ESCC was similar to the distribution of xCT. (a, b magnification ×200, c magnification ×400). d A correlation analysis of the relationships between the xCT and Ki-67 positivity rates was performed by producing Fit Y by X plots. The xCT positivity rate was positively correlated with the Ki-67 labeling index ($R^2 = 0.117$, $p = 0.0038$)

0.037, and 0.035, respectively) (Table 3). These findings suggested that xCT expression was induced in ESCC and that the xCT positivity rate is related to prognosis.

## Discussion

xCT is a component of a plasma membrane transporter, system xc-, that mediates the cellular uptake of extracellular cystine in exchange for intracellular glutamate and thereby plays a key role in GSH synthesis. Previous studies have detected increased xCT expression in a broad range of cancer cell lines [5–12]. The activity of xCT-mediated cystine uptake in cancer cells is strongly associated with cell proliferation and tumor growth [3, 17]. The inhibition of xCT has been demonstrated to suppress the growth of a variety of carcinomas both in vitro and in vivo [5, 7, 8]. In ESCC, Chen et al. [12] showed that sulfasalazine (SASP), a pharmacological inhibitor of system xc-, inhibited the growth of KYSE150, an ESCC cell line, in a dose-dependent manner. In the present study, we showed that knocking down xCT with xCT siRNA significantly inhibited cell cycle progression and proliferation in the ESCC cell lines TE13 and KYSE170. These reports and our results suggest that xCT plays an important role in tumor growth and could be used as a target of cancer therapy.

**Table 1** Correlations between clinicopathological parameters and xCT expression

| Variables | xCT positivity rate | | *p* value |
|---|---|---|---|
| | <20 % ($n = 35$) | ≥20 % ($n = 35$) | |
| pT | | | |
| pT1 | 15 | 17 | 0.811 |
| pT2-3 | 20 | 18 | |
| pN | | | |
| Negative | 19 | 13 | 0.230 |
| Positive | 16 | 22 | |
| pStage | | | |
| 0–II | 25 | 19 | 0.216 |
| III–IV | 10 | 16 | |
| Histological type | | | |
| Differentiated type SCC | 23 | 26 | 0.603 |
| Poorly differentiated type SCC | 12 | 9 | |
| Lymphatic invasion | | | |
| Negative | 15 | 17 | 0.811 |
| Positive | 20 | 18 | |
| Venous invasion | | | |
| Negative | 21 | 18 | 0.631 |
| Positive | 14 | 17 | |

*pT* pathological T stage, *pN* pathological N stage, *pStage* pathological stage, *SCC* squamous cell carcinoma

* $p < 0.05$ Fisher's exact test

**Table 2** 5-year survival rate of esophageal cancer according to clinicopathological features

| Variables | 5-year survival rate (%) | *p* value |
|---|---|---|
| pT | | |
| pT1 | 81.8 | 0.004* |
| pT2-3 | 52.1 | |
| pN | | |
| Negative | 82.3 | 0.005* |
| Positive | 51.1 | |
| pStage | | |
| 0–II | 74.7 | 0.012* |
| III–IV | 51.8 | |
| Histological type | | |
| Differentiated type SCC | 74.3 | 0.093 |
| Poorly differentiated type SCC | 49.0 | |
| Lymphatic invasion | | |
| Negative | 78.2 | 0.017* |
| Positive | 56.0 | |
| Venous invasion | | |
| Negative | 77.6 | 0.028* |
| Positive | 50.6 | |
| Ki-67 labeling index | | |
| <35 % | 74.5 | 0.007* |
| ≥35 % | 40.7 | |
| xCT positive rate | | |
| <20 % | 76.2 | 0.056 |
| ≥20 % | 56.8 | |

*pT* pathological T stage, *pN* pathological N stage, *pStage* pathological stage, *SCC* squamous cell carcinoma

* $p < 0.05$ the log-rank test

Several studies have investigated the mechanism by which xCT regulates cell cycle progression. Lastro et al. [18] showed that xCT directly affects cell cycle progression at the $G_1$-S phase through the regulation of AP-1 transcription factor activity. Chen et al. [12] showed that SASP downregulated b-catenin-mediated transcriptional activity and cyclin D1 expression, implying that suppression of the canonical Wnt signaling pathway contributes to the inhibition of cell cycle progression by SASP. Ishimoto et al. [11] showed that CD44 ablation suppressed gastric tumor growth in a mouse model of spontaneous tumorigenesis concomitant with the upregulation of $p38^{MAPK}$ phosphorylation and $p21^{CIP1/WAF1}$ gene expression, and that treatment with the specific xCT inhibitor SASP induced $p38^{MAPK}$ activation and suppressed CD44-dependent tumor growth in a xenograft model. To determine how the downregulation of xCT affects cell proliferation, we used a bioinformatics approach to analyze the genome-wide consequences of xCT knockdown. Microarray analysis showed that among the 1652 genes that displayed changes in their expression levels after xCT knockdown, 248 had cell proliferation related functions (data not shown). Furthermore, many of these genes were well connected in the top-ranked signaling network (Supplementary Fig. 2), indicating that they are not only functionally related but are also regulated together at the expression level by xCT-related signal transduction pathways. Cancer was one of the top-ranked diseases associated with xCT-related genes, and $G_1$/S checkpoint regulation was one of the top-ranked canonical pathways related to xCT (Supplementary Table 3).

Regarding signaling networks, we noted that the expression levels of several $G_1$/S checkpoint related genes, such as TP53INP1, CDKN1A ($p21^{CIP1/WAF1}$), cyclin D1/cdk4, and E2F5 were altered by the knocking down of xCT (Supplementary Fig. 2). xCT-mediated cystine transport for GSH synthesis plays a key role in the prevention of oxidative stress signaling. Oxidative stress has been implicated in p53-$p21^{CIP1/WAF1}$ signaling, and consequently, in cell cycle regulation [19]. $p21^{CIP1/WAF1}$ is a cyclin-dependent kinase inhibitor that directly inhibits the activity of cyclin D1/CDK4 complex. The active cyclin D1/CDK4 complex targets the retinoblastoma protein for

Table 3 Prognostic factors for esophageal cancer according to multivariate analysis

| Variables | Risk ratio | 95 % CI | *p* value |
|---|---|---|---|
| pT | | | |
| pT1 | 3.397 | 0.942–15.029 | 0.063 |
| pT2-3 | | | |
| pN | | | |
| Negative | 1.596 | 0.365–7.203 | 0.533 |
| Positive | | | |
| pStage | | | |
| 0–II | 0.855 | 0.191–3.752 | 0.834 |
| III–IV | | | |
| Histological type | | | |
| Differentiated type SCC | 2.491 | 0.763–7.953 | 0.129 |
| Poorly differentiated type SCC | | | |
| Lymphatic invasion | | | |
| Negative | 2.314 | 0.900–6.976 | 0.083 |
| Positive | | | |
| Venous invasion | | | |
| Negative | 4.262 | 1.403–14.810 | 0.010* |
| Positive | | | |
| Ki-67 labeling index | | | |
| <35 % | 3.000 | 1.071–8.439 | 0.037* |
| ≥35 % | | | |
| xCT positive rate | | | |
| <20 % | 2.746 | 1.072–7.720 | 0.035* |
| ≥20 % | | | |

*pT* pathological T stage, *pN* pathological N stage, *SCC* squamous cell carcinoma, CI 95 % confidence interval

* $p < 0.05$ Cox's proportional hazards model 95 % *CI*

phosphorylation, allowing the release of E2F transcription factors that activate $G_1$-S phase gene expression [20]. However, our results showed expressions of these genes were changed by the knocking down of xCT regardless of the mutation status of TP53 (The mutation status of TP53 exon 5-8 determined by direct sequencing showed that TE13 cells had wild-type, and KYSE170 cells had mutation.) [21]. Further, in our data, although the knocking down of xCT inhibited $G_1$/S cell cycle progression, gene expressions of TP53INP1 and $p21^{CIP1/WAF1}$ were significantly decreased, suggesting the effect of negative feedback. These observations suggest that xCT may controls the $G_1$/S checkpoint via the direct regulation of downstream factors, such as cyclin D1/cdk4 and E2F, without passing through p53-$p21^{CIP1/WAF1}$ signaling pathway.

Our immunofluorescent staining of ESCC cell lines and immunohistochemical analysis of human ESCC samples revealed that xCT was predominantly distributed in the nuclei of ESCC cells. In general, system xc- is known to function as the exchange system for cystine/glutamate in the cell membrane. The nuclear localization of several cell membrane proteins is known to be correlated with oncogenic transformation and cell proliferation [22–24], suggesting that changes in the intracellular localization of several molecules are correlated with cancer development. Our results regarding the nuclear expression of xCT and our gene expression profile findings indicate that xCT functions as not only a cystine/glutamate exchanger but also as a transcriptional regulator in cancer cells. We showed that knocking down of xCT significantly decreased the gene expression of E2F5 which belongs to the E2F transcription factor family [25, 26]. Although the functional roles of E2F5 have still to be fully characterized, Umemura et al. [27] reported that the overexpression of E2F5 is correlated with an aggressive pathology in certain breast cancer subtypes. In the present study, E2F5 was the fourth most downregulated gene (fold change: −3.18) in the xCT siRNA transfected TE13 cells (Supplementary Table 2). One possible mechanism and meaning of the distribution of xCT in ESCC may be explained by the regulation of this transcriptional factor. Although the significance of xCT expression in the nuclear region in ESCC should be verified by further studies, these observations suggest that xCT may act as a novel regulator of E2F5 in ESCC.

The clinical significance of xCT expression in cancer tissue remains to be fully elucidated. As far as we know, there have ever been no reports to investigate the correction between xCT expression and clinicopathological features in ESCC patients. Peters et al. [28] examined the gene expression profile of esophageal adenocarcinoma and showed that the expression levels of 270 genes were significantly associated with the number of involved lymph nodes, and xCT was one of these genes. In the present study, multivariable analysis demonstrated that xCT expression was an independent prognostic factor for ESCC. Although no correlation was found between the xCT positivity rate and any other clinicopathological parameter, our observations indicate that xCT may have prognostic effect on ESCC patients via the regulation of $G_1$/S checkpoint transcriptional factors, suggesting that it might be a useful indicator for selecting the postoperative treatment approach.

In summary, we have found that xCT plays a role in the proliferation of ESCC cells. As far as we know, this is the first report to analyze the gene expression profiles of xCT siRNA transfected ESCC cells in microarray, and investigate the clinicopathological and prognostic significance of xCT expression in an immunohistochemical analysis of human ESCC samples. Microarray analyses showed that xCT siRNA transfection changed the expression levels of genes related to $G_1$/S cell cycle progression, including

TP53INP1, CDKN1A, CyclinD1/cdk4, and E2F5. Furthermore, immunohistochemical staining showed that xCT expression is an independent prognostic factor of ESCC patients. A deeper understanding of the role of xCT might lead to it being used as an important biomarker of tumor development and/or a novel therapeutic target for ESCC.

**Acknowledgments** . This work was supported by Grants-in-Aid for Young Scientists (B) (22791295, 23791557, 24791440), a Grant-in-Aid for Scientific Research (C) (22591464, 24591957) from the Japan Society for the Promotion of Science.

**Conflict of interest** The authors declare that they have no conflict of interest.

## References

1. Sato H, Tamba M, Ishii T, Bannai S. Cloning and expression of a plasma membrane cystine/glutamate exchange transporter composed of two distinct proteins. J Biol Chem. 1999;274:11455–8.
2. Sato H, Tamba M, Kuriyama-Matsumura K, Okuno S, Bannai S. Molecular cloning and expression of human xCT, the light chain of amino acid transport system xc. Antioxid Redox Signal. 2000;2:665–71.
3. Lo M, Wang YZ, Gout PW. The x(c)- cystine/glutamate antiporter: a potential target for therapy of cancer and other diseases. J Cell Physiol. 2008;215:593–602.
4. Kim JY, Kanai Y, Chairoungdua A, Cha SH, Matsuo H, Kim DK, et al. Human cystine/glutamate transporter: cDNA cloning and upregulation by oxidative stress in glioma cells. Biochim Biophys Acta. 2001;1512:335–44.
5. Chung WJ, Lyons SA, Nelson GM, Hamza H, Gladson CL, Gillespie GY, et al. Inhibition of cystine uptake disrupts the growth of primary brain tumors. J Neurosci. 2005;25:7101–10.
6. Bassi MT, Gasol E, Manzoni M, Pineda M, Riboni M, Martín R, et al. Identification and characterisation of human xCT that co-expresses, with 4F2 heavy chain, the amino acid transport activity system xc-. Pflugers Arch. 2001;442:286–96.
7. Narang VS, Pauletti GM, Gout PW, Buckley DJ, Buckley AR. Suppression of cystine uptake by sulfasalazine inhibits proliferation of human mammary carcinoma cells. Anticancer Res. 2003;23:4571–9.
8. Doxsee DW, Gout PW, Kurita T, Lo M, Buckley AR, Wang Y, et al. Sulfasalazine-induced cystine starvation: potential use for prostate cancer therapy. Prostate. 2007;67:162–71.
9. Okuno S, Sato H, Kuriyama-Matsumura K, Tamba M, Wang H, Sohda S, et al. Role of cystine transport in intracellular glutathione level and cisplatin resistance in human ovarian cancer cell lines. Br J Cancer. 2003;88:951–6.
10. Lo M, Ling V, Low C, Wang YZ, Gout PW. Potential use of the anti-inflammatory drug, sulfasalazine, for targeted therapy of pancreatic cancer. Curr Oncol. 2010;17:9–16.
11. Ishimoto T, Nagano O, Yae T, Tamada M, Motohara T, Oshima H, et al. CD44 variant regulates redox status in cancer cells by stabilizing the xCT subunit of system xc(−) and thereby promotes tumor growth. Cancer Cell. 2011;19:387–400.
12. Chen RS, Song YM, Zhou ZY, Tong T, Li Y, Fu M, et al. Disruption of xCT inhibits cancer cell metastasis via the caveolin-1/beta-catenin pathway. Oncogene. 2009;28:599–609.
13. Lyons SA, Chung WJ, Weaver AK, Ogunrinu T, Sontheimer H. Autocrine glutamate signaling promotes glioma cell invasion. Cancer Res. 2007;67:9463–71.
14. Nishihira T, Hashimoto Y, Katayama M, Mori S, Kuroki T. Molecular and cellular features of esophageal cancer cells. J Cancer Res Clin Oncol. 1993;119:441–9.
15. Shimada Y, Imamura M, Wagata T, Yamaguchi N, Tobe T. Characterization of 21 newly established esophageal cancer cell lines. Cancer. 1992;69:277–84.
16. Sobin L, Gospodarowicz M, Wittekind C, editors. TNM Classification of malignant tumors. 7th ed. Hoboken: Wiley; 2009.
17. Gout PW, Buckley AR, Simms CR, Bruchovsky N. Sulfasalazine, a potent suppressor of lymphoma growth by inhibition of the x(c)- cystine transporter: a new action for an old drug. Leukemia. 2001;15:1633–40.
18. Lastro M, Kourtidis A, Farley K, Conklin DS. xCT expression reduces the early cell cycle requirement for calcium signaling. Cell Signal. 2008;20:390–9.
19. Muller M. Cellular senescence: molecular mechanisms, in vivo significance, and redox considerations. Antioxid Redox Signal. 2009;11:59–98.
20. Lukas J, Bartkova J, Bartek J. Convergence of mitogenic signalling cascades from diverse classes of receptors at the cyclin D-cyclin-dependent kinase-pRb-controlled G1 checkpoint. Mol Cell Biol. 1996;16:6917–25.
21. Komatsu S, Imoto I, Tsuda H, Kozaki KI, Muramatsu T, Shimada Y, et al. Overexpression of SMYD2 relates to tumor cell proliferation and malignant outcome of esophageal squamous cell carcinoma. Carcinogenesis. 2009;30:1139–46.
22. Islas S, Vega J, Ponce L, González-Mariscal L. Nuclear localization of the tight junction protein ZO-2 in epithelial cells. Exp Cell Res. 2002;274:138–48.
23. Gottardi CJ, Arpin M, Fanning AS, Louvard D. The junction-associated protein, zonula occludens-1, localizes to the nucleus before the maturation and during the remodeling of cell–cell contacts. Proc Natl Acad Sci USA. 1996;93:10779–84.
24. Dhawan P, Singh AB, Deane NG, No Y, Shiou SR, Schmidt C, et al. Claudin-1 regulates cellular transformation and metastatic behavior in colon cancer. J Clin Invest. 2005;115:1765–76.
25. La Thangue NB, Rigby PW. An adenovirus E1A-like transcription factor is regulated during the differentiation of murine embryonal carcinoma stem cells. Cell. 1987;49:507–13.
26. Dyson N. The regulation of E2F by pRB-family proteins. Genes Dev. 1998;12:2245–62.
27. Umemura S, Shirane M, Takekoshi S, Kusakabe T, Itoh J, Egashira N, et al. Overexpression of E2F–5 correlates with a pathological basal phenotype and a worse clinical outcome. Br J Cancer. 2009;100:764–71.
28. Peters CJ, Rees JR, Hardwick RH, Hardwick JS, Vowler SL, Ong CA, Oesophageal Cancer Clinical and Molecular Stratification (OCCAMS) Study Group, et al. A 4-gene signature predicts survival of patients with resected adenocarcinoma of the esophagus, junction, and gastric cardia. Gastroenterology. 2010;139 (1995–2004):e15.

Hindawi Publishing Corporation
BioMed Research International
Volume 2014, Article ID 936401, 12 pages
http://dx.doi.org/10.1155/2014/936401

Hindawi

*Research Article*

# The K–Cl Cotransporter KCC3 as an Independent Prognostic Factor in Human Esophageal Squamous Cell Carcinoma

**Atsushi Shiozaki,[1] Kenichi Takemoto,[1] Daisuke Ichikawa,[1] Hitoshi Fujiwara,[1] Hirotaka Konishi,[1] Toshiyuki Kosuga,[1] Shuhei Komatsu,[1] Kazuma Okamoto,[1] Mitsuo Kishimoto,[2] Yoshinori Marunaka,[3,4] and Eigo Otsuji[1]**

[1] *Division of Digestive Surgery, Department of Surgery, Kyoto Prefectural University of Medicine, 465 Kajii-cho, Kamigyo-ku, Kyoto 602-8566, Japan*
[2] *Department of Pathology, Kyoto Prefectural University of Medicine, Kyoto 602-8566, Japan*
[3] *Departments of Molecular Cell Physiology and Bio-Ionomics, Graduate School of Medical Science, Kyoto Prefectural University of Medicine, Kyoto 602-8566, Japan*
[4] *Japan Institute for Food Education and Health, St. Agnes' University, Kyoto 602-8013, Japan*

Correspondence should be addressed to Atsushi Shiozaki; shiozaki@koto.kpu-m.ac.jp

Received 22 May 2014; Accepted 16 June 2014; Published 9 July 2014

Academic Editor: Akio Tomoda



The objectives of the present study were to investigate the role of K–Cl cotransporter 3 (KCC3) in the regulation of cellular invasion and the clinicopathological significance of its expression in esophageal squamous cell carcinoma (ESCC). Immunohistochemical analysis performed on 70 primary tumor samples obtained from ESCC patients showed that KCC3 was primarily found in the cytoplasm of carcinoma cells. Although the expression of KCC3 in the main tumor (MT) was related to several clinicopathological features, such as the pT and pN categories, it had no prognostic impact. KCC3 expression scores were compared between the MT and cancer nest (CN), and the survival rate of patients with a CN > MT score was lower than that of patients with a CN ≤ MT score. In addition, the survival rate of patients in whom KCC3 was expressed in the invasive front of tumor was lower than that of the patients without it. Furthermore, multivariate analysis demonstrated that the expression of KCC3 in the invasive front was one of the most important independent prognostic factors. The depletion of KCC3 using siRNAs inhibited cell migration and invasion in human ESCC cell lines. These results suggest that the expression of KCC3 in ESCC may affect cellular invasion and be related to a worse prognosis in patients with ESCC.

## 1. Introduction

The K–Cl cotransporter (KCC) mediates the coupled movement of $K^+$ and $Cl^-$ ions across the plasma membrane and is involved in the regulation of cell volume, transepithelial ion transport, and maintenance of intracellular $Cl^-$ concentrations ($[Cl^-]_i$) [1, 2]. Four isoforms of the KCC have been identified and are termed KCC1, KCC2, KCC3, and KCC4 [3]. The four KCC isoforms share a common protein structure with 12 transmembrane regions in a central hydrophobic domain, together with hydrophilic N- and C-termini that may be cytoplasmic [4]. Although the expression of KCC1 is reportedly ubiquitous [5], that of KCC2 is restricted to neurons in the central nervous system [6]. KCC3 is expressed in the muscle, brain, lung, heart, and kidney [7], and KCC4 transcripts are the most abundant in the heart and kidney [4].

Several recent studies described the important roles of KCC in cancer development, tumor invasion, and possibly metastasis [8–11]. KCC3 was found to be important for cell-cycle progression, migration, and invasion in cervical carcinoma, ovarian cancer, breast cancer, and glioma [8, 9, 12, 13]. In addition, the overexpression of KCC3 downregulated the formation of the E-cadherin/$\beta$-catenin complex, and the subsequent upregulation of KCl cotransport activity was

shown to benefit cancer cells in the epithelial-mesenchymal transition (EMT) [8]. However, the roles of KCC3 in the invasion of esophageal squamous cell carcinoma (ESCC) cells remain uncertain. Furthermore, the clinicopathological meaning of the expression of KCC3 in human ESCCs has not yet been evaluated.

The objectives of the present study were to investigate the roles of KCC3 in the cell migration and invasion of ESCC. Furthermore, we analyzed the expression of KCC3 in human ESCC samples and determined its relationships with the clinicopathological features and prognosis of ESCC patients. Our results revealed the important role of KCC3 in the tumor progression of ESCC.

## 2. Materials and Methods

*2.1. Patients and Primary Tissue Samples.* ESCC tumor samples were obtained from 70 patients with histologically proven primary ESCC who underwent esophagectomy (potentially curative R0 resection) at Kyoto Prefectural University of Medicine (Kyoto, Japan) between 1998 and 2007 and were analyzed retrospectively. These samples were embedded in paraffin 24 h after being fixed in formalin. Patient eligibility criteria included not having developed synchronous tumors or multiple metachronous tumors and not having received preoperative chemotherapy or radiation therapy. We excluded patients with noncuratively resected tumors or nonconsecutive data. All patients gave their written informed consent for inclusion in this study. Relevant clinicopathological and survival data were obtained from the hospital database. Staging was principally based on the seventh TNM staging system [14].

*2.2. Immunohistochemistry.* Paraffin sections (3 $\mu$m thick) of tumor tissue were subjected to immunohistochemical staining for KCC3 using the avidin-biotin-peroxidase method. Briefly, paraffin sections were dewaxed in xylene and hydrated through a graded series of alcohols. Antigen retrieval was performed by heating the samples in Dako REAL Target Retrieval Solution (Glostrup, Denmark) for 40 min at 95°C. Endogenous peroxidase activity was quenched by incubating the sections for 30 min in 0.3% $H_2O_2$. Sections were incubated for one hour at room temperature with the following antibody: the KCC3 antibody (HPA034563; Atlas Antibodies AB, Stockholm, Sweden). The avidin-biotin-peroxidase complex system (Vectastain ABC Elite kit; Vector Laboratories, Burlingame, CA, USA) was used for color development with diaminobenzidine tetrahydrochloride. Sections were counterstained with hematoxylin. These sections were then dehydrated through a graded series of alcohols, cleared in xylene, and mounted. Control sections of known positive ESCC were included in each antibody run, and negative control sections were produced by omitting the primary antibody.

Immunohistochemical samples stained with KCC3 were graded semiquantitatively by considering both the staining intensity and percentage of positive tumor cells using an immunoreactive score (IRS) [15]. Staining intensity was scored as 0 (no staining), 1 (weak staining), 2 (moderate staining), or 3 (strong staining). The proportion of positive tumor cells was scored from 0 to 1.0. The score of each sample was calculated as the maximum multiplied product of the intensity and proportion scores (0 to 3.0).

*2.3. Cell Culture.* The human ESCC cell lines TE5 and TE9 were obtained from the Cell Resource Center for Biomedical Research at the Institute of Development, Aging, and Cancer (Tohoku University, Sendai, Japan) [16]. These cells were grown in RPMI-1640 medium (Nacalai Tesque, Kyoto, Japan) supplemented with 100 U/mL of penicillin, 100 $\mu$g/mL of streptomycin, and 10% fetal bovine serum (FBS). Cells were cultured in flasks or dishes in a humidified incubator at 37°C under 5% $CO_2$ in air.

*2.4. Small Interfering RNA (siRNA) Transfection.* Cells were transfected with 10 nmol/L KCC3 siRNA (Stealth RNAi siRNA #HSS HSS115159, HSS190762, HSS190763; Invitrogen, Carlsbad, CA) using the Lipofectamine RNAiMAX reagent (Invitrogen), according to the manufacturer's instructions. The medium containing siRNA was replaced with fresh medium after 24 h. We used three independent KCC3 siRNAs to exclude off target effects. The control siRNA provided (Stealth RNAi siRNA Negative Control; Invitrogen) was used as a negative control.

*2.5. Real-Time Reverse Transcription-Polymerase Chain Reaction (RT-PCR).* Total RNA was extracted using an RNeasy kit (Qiagen, Valencia, CA). Messenger RNA (mRNA) expression was measured by quantitative real-time PCR (7300 Real-Time PCR System; Applied Biosystems, Foster City, CA) with TaqMan Gene Expression Assays (Applied Biosystems), according to the manufacturer's instructions. Expression levels were measured for the following gene: KCC3 (Hs00994548_m1) (Applied Biosystems). Expression was normalized for the KCC3 gene to the housekeeping gene beta-actin (ACTB, Hs01060665_g1; Applied Biosystems). Assays were performed in duplicate.

*2.6. Analysis of Cell Migration and Invasion.* The migration assay was conducted using a Cell Culture Insert with a pore size of 8 $\mu$m (BD Biosciences, Bedford, MA). Biocoat Matrigel (BD Biosciences) was used to evaluate cell invasion potential. Briefly, cells ($1.5 \times 10^5$ cells per well) were seeded in the upper chamber in serum-free medium 24 h after siRNA transfection. The lower chamber contained medium with 10% FBS. The chambers were incubated for 48 h at 37°C in 5% $CO_2$, and nonmigrated or noninvaded cells were then removed from the upper side of the membrane by scrubbing with cotton swabs. Migrated or invaded cells were fixed on the membrane and stained with Diff-Quick staining reagents (Sysmex, Kobe, Japan). The migrated or invaded cells on the lower side of the membrane were counted in four independent fields of view at 100x magnification of each insert. Each assay was performed in triplicate.

*2.7. Statistical Analysis.* Statistical analysis was carried out using Fisher's exact test to investigate correlations between clinicopathological parameters and KCC3 expression.

Survival curves were constructed using the Kaplan-Meier method, and differences in survival were examined using the log-rank test. Multivariate analysis of the factors influencing survival was performed using the Cox proportional hazard model. Multiple comparisons were carried out using Dunnett's test after one-way ANOVA. Differences were considered significant when the associated $P$ value was less than 0.05. All analyses were performed using statistical software (JMP, version 10; SAS Institute Inc., Cary, NC, USA). Correlation analyses were performed by creating Fit $Y$ by $X$ plots using JMP.

## 3. Results

*3.1. KCC3 Protein Expression in Human ESCCs.* An immunohistochemical investigation with the KCC3 antibody revealed the expression of KCC3 in the parabasal cell layer of normal esophageal mucosa (Figure 1(a)). We examined the expression of KCC3 in 70 primary tumor samples of human ESCC based on their immunohistochemical reactivity. The KCC3 protein was mostly expressed in the cytoplasm of carcinoma cells (Figure 1(b)). The KCC3 score in the main tumor (MT) varied widely between the tumors. The minimum KCC3 score was 0 while the maximum KCC3 score was 2.4 in MT (median = 0.725; mean ± standard error of the mean (SEM) = 0.780 ± 0.072). Regarding the expression of KCC3 in MT, we divided ESCC patients into 2 groups using the median staining score: a low grade KCC3 expression group with staining scores ≤0.725, $n = 35$, and a high grade KCC3 expression group with staining scores >0.725, $n = 35$. Figures 1(c) and 1(d) show the representative histopathological findings of low or high KCC3 expression samples. Correlations between the expression of KCC3 in MT and various clinicopathological parameters were analyzed (Table 1). We found correlations between the expression of KCC3 in MT and location of the primary tumor, the pT or pN category (Table 1).

We then focused on the expression of KCC3 in the cancer nest (CN) of ESCC (Figure 1(e)) and analyzed the KCC3 score in CN. The minimum KCC3 score was 0, and the maximum KCC3 score was 2.6 in CN (median = 1.000; mean ± SEM = 1.087 ± 0.096). The KCC3 score in CN was positively correlated with the KCC3 score in MT ($R^2 = 0.3388$, $P < 0.0001$) (Figure 2). Regarding the expression of KCC3 in CN, we divided ESCC patients into 2 groups using the median staining score, a low grade KCC3 expression group with staining scores ≤1.000, $n = 36$, and a high grade KCC3 expression group with staining scores >1.000, $n = 34$, and compared their clinicopathological features (Table 1). A correlation was found between the expression of KCC3 in CN and location of the primary tumor (Table 2). Regarding the comparison of KCC3 scores between MT and CN in each sample, we divided ESCC patients into 2 groups, CN > MT, $n = 39$, and CN ≤ MT, $n = 31$, and compared their clinicopathological features (Table 1). A correlation was not found between the comparison of KCC3 scores and clinicopathological features (Table 1).

Furthermore, we analyzed the localization of KCC3 expression in tumors. In 48 cases, the expression of KCC3 was found in the invasive front of the tumor (Figure 1(f)). Regarding the expression of KCC3 in the invasive front of the tumor, we divided ESCC patients into 2 groups, negative ($n = 22$) and positive ($n = 48$), and compared their clinicopathological features (Table 2). A correlation was found between the expression of KCC3 in the invasive front and the MT score, CN score, or their comparison (CN/MT) (Table 2). No correlation was found between the expression of KCC3 in the invasive front and any other clinicopathological parameter (Table 2).

*3.2. Prognostic Impact of KCC3 Protein Expression for Patients with ESCC.* We determined the prognostic impact of the expression of KCC3 for patients with ESCC. Regarding the expression of KCC3 in MT, no significant difference was observed in the 5-year survival rate between patients with the high grade expression of KCC3 and those with the low grade expression of KCC3 in MT (Figure 3(a)). Similarly, no significant differences were observed in the 5-year survival rate between patients with the high grade expression of KCC3 and those with the low grade expression of KCC3 in CN (Figure 3(b)). Regarding comparisons of KCC3 score, the 5-year survival rate of the patients with CN > MT (55.5%) was lower than that of patients with CN ≤ MT (76.7%) ($P = 0.133$) (Figure 3(c)). The 5-year survival rate of the patients with KCC3 expression in the invasive front (57.1%) was lower than that of the patients without it (81.8%), although there was no statistical difference ($P = 0.089$) (Figure 3(d)). Interestingly, when patients were divided into 2 groups, CN > MT and invasive front positive, $n = 31$, and others, $n = 39$, the 5-year survival rate of patients with CN > MT and invasive front positive (46.1%) was significantly lower than that of other patients (79.0%) ($P = 0.022$) (Figure 3(e)).

Furthermore, we assessed which of the 13 variables studied (age, gender, location of the primary tumor, histological type, tumor size, lymphatic invasion, venous invasion, pT and pN category, KCC3 score in MT, KCC3 score in CN and CN/MT, and KCC3 expression in the invasive front) influenced survival following curative resection of esophageal cancer. Univariate analysis of survival after esophagectomy revealed that lymphatic invasion, venous invasion, and the pT and pN categories were found to be significant prognostic factors ($P = 0.017$, 0.017, 0.002, and 0.003, resp.) (Table 3). Multivariate analysis with variables whose $P$ values were less than 0.100 in univariate analysis demonstrated that lymphatic invasion, pT and pN category, and KCC3 expression in invasive front were independent prognostic factors ($P = 0.044$, 0.015, 0.011, and 0.001, resp.) (Table 4). KCC3 expression in invasive front was the strongest prognostic factor of all clinicopathological features. These findings suggest that the expression of KCC3 might be a valuable prognostic factor for patients with ESCC.

*3.3. KCC3 Controlled Cell Migration and Invasion in ESCC Cells.* We conducted knockdown experiments with KCC3 siRNA in ESCC cells and analyzed the effects of KCC3 knockdown on cell migration and invasion. We used three independent KCC3 siRNAs to exclude off target effects. All three KCC3 siRNAs effectively reduced KCC3 mRNA levels

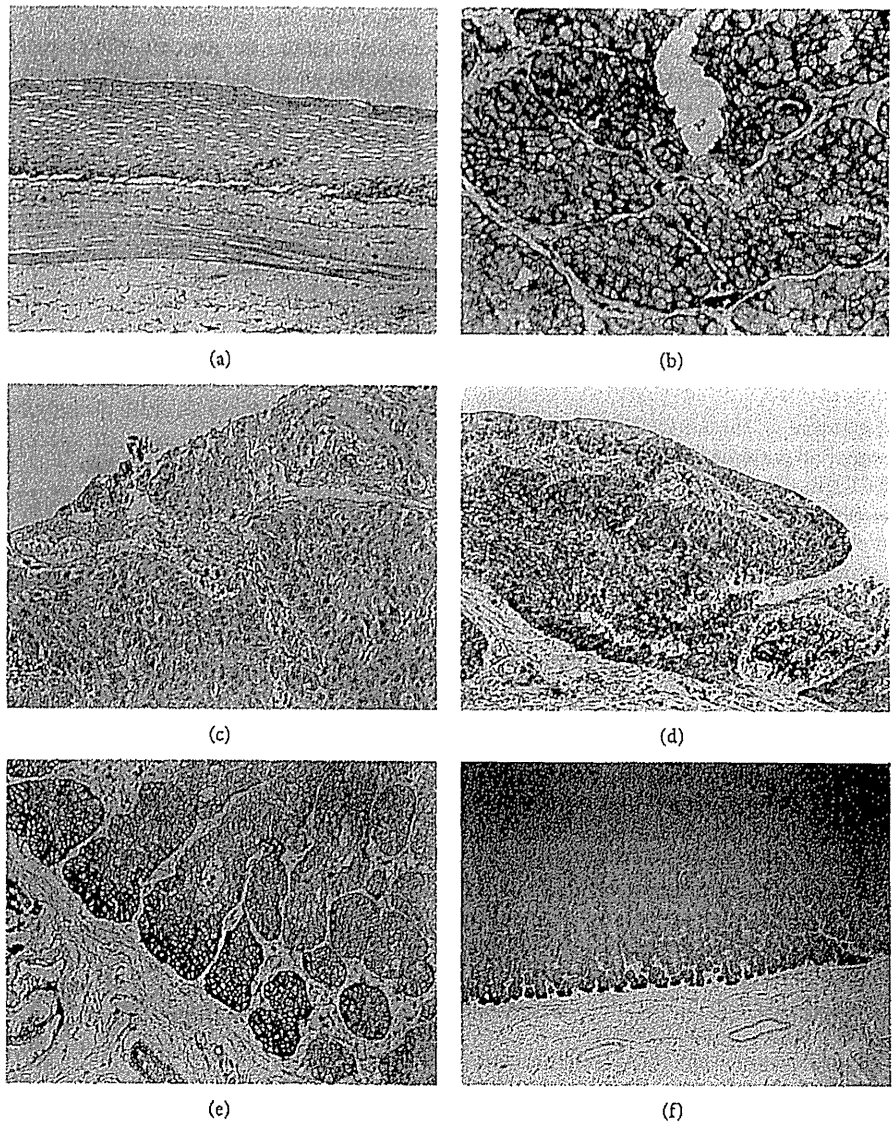


FIGURE 1: KCC3 protein expression in human esophageal squamous cell carcinoma (ESCC). (a) Immunohistochemical staining of noncancerous esophageal epithelia with the KCC3 antibody. Magnification: ×200. (b) Immunohistochemical staining of primary human ESCC samples with the KCC3 antibody. Magnification: ×400. (c) Immunohistochemical staining of primary human ESCC samples with the low grade expression of KCC3 in the main tumor (MT). Magnification: ×200. (d) Immunohistochemical staining of primary human ESCC samples with the high grade expression of KCC3 in the main tumor (MT). Magnification: ×200. (e) Immunohistochemical staining of primary human ESCC samples with the high grade expression of KCC3 in the cancer nest (CN). Magnification: ×200. (f) Immunohistochemical staining of primary human ESCC samples that expressed KCC3 in the invasive front of the tumor. Magnification: ×40.

in both TE5 and TE9 cells (Figure 4(a)). In TE5 cells, all three KCC3 siRNAs significantly inhibited cell migration and invasion (Figure 4(b)). In TE9 cell, downregulation of KCC3 inhibited cell migration and invasion, too (Figure 4(c)). These results suggest that KCC3 plays an important role in regulating cell migration and invasion in ESCC cells.

## 4. Discussion

Recent studies have shown that ion channels and transporters play crucial roles in cellular functions, and their roles have been studied in cancer cells [17, 18]. Various types of ion channels, such as voltage-gated $K^+$ channels, voltage-gated HERG channels, $Ca_2^+$ channels, and transient receptor potential channels, have been found to be expressed in gastrointestinal cancer cells and tissues and to regulate tumor behavior [19–22]. Regulators of intracellular pH such as anion exchanger, sodium-hydrogen exchanger, and carbonic anhydrases also related to tumor development of gastrointestinal cancer cells [23–25]. Furthermore, several reports have indicated that $Cl^-$ channels/transporters, such as $Cl^-$ channels, chloride intracellular channel (CLIC), KCC, and NKCC, play crucial

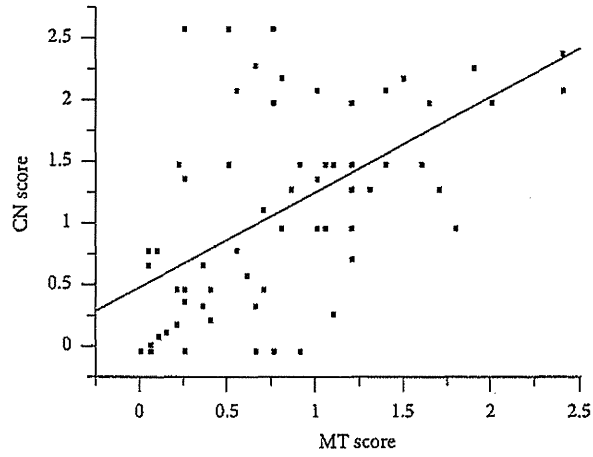


FIGURE 2: A correlation analysis of the relationship between the KCC3 score in main tumor (MT) and KCC3 score in the cancer nest (CN) was performed by producing Fit $Y$ by $X$ plots. The KCC3 score in CN was positively correlated with the KCC3 score in MT ($R^2$ = 0.3388, $P < 0.0001$).

TABLE 1: Relationships between the clinicopathological features of esophageal cancer and expression of KCC3 in the main tumor or cancer nest.

| Variable | MT | | | CN | | | CN/MT | | |
|---|---|---|---|---|---|---|---|---|---|
| | Low ($n = 35$) | High ($n = 35$) | $P$ value | Low ($n = 36$) | High ($n = 34$) | $P$ value | CN ≤ MT ($n = 31$) | CN > MT ($n = 39$) | $P$ value |
| Age | | | | | | | | | |
| <60 years | 11 | 11 | 1.000 | 11 | 11 | 1.000 | 6 | 16 | 0.071 |
| ≥60 years | 24 | 24 | | 25 | 23 | | 25 | 23 | |
| Gender | | | | | | | | | |
| Male | 30 | 29 | 1.000 | 30 | 29 | 1.000 | 25 | 34 | 0.520 |
| Female | 5 | 6 | | 6 | 5 | | 6 | 5 | |
| Location of the primary tumor | | | | | | | | | |
| Ut-Mt | 18 | 29 | 0.0101* | 19 | 28 | 0.0112* | 21 | 26 | 1.000 |
| Lt-Ae | 17 | 6 | | 17 | 6 | | 10 | 13 | |
| Histological type | | | | | | | | | |
| Well/moderately differentiated SCC | 22 | 27 | 0.297 | 26 | 23 | 0.796 | 22 | 27 | 1.000 |
| Poorly differentiated SCC | 13 | 8 | | 10 | 11 | | 9 | 12 | |
| Tumor size | | | | | | | | | |
| <50 mm | 22 | 27 | 0.2968 | 24 | 25 | 0.6069 | 24 | 25 | 0.2967 |
| ≥50 mm | 13 | 8 | | 12 | 9 | | 7 | 14 | |
| Lymphatic invasion | | | | | | | | | |
| Negative | 15 | 18 | 0.6324 | 20 | 13 | 0.1606 | 18 | 15 | 0.1482 |
| Positive | 20 | 17 | | 16 | 21 | | 13 | 24 | |
| Venous invasion | | | | | | | | | |
| Negative | 19 | 21 | 0.8094 | 20 | 20 | 0.8133 | 18 | 22 | 1.000 |
| Positive | 16 | 14 | | 16 | 14 | | 13 | 17 | |
| pT | | | | | | | | | |
| pT1 | 10 | 23 | 0.0037* | 14 | 19 | 0.2309 | 18 | 15 | 0.1482 |
| pT2-3 | 25 | 12 | | 22 | 15 | | 13 | 24 | |
| pN | | | | | | | | | |
| pN0 | 11 | 22 | 0.0160* | 15 | 18 | 0.473 | 16 | 17 | 0.631 |
| pN1-3 | 24 | 13 | | 21 | 16 | | 15 | 22 | |

MT: main tumor; CN: cancer nest; Ut: upper thoracic esophagus; Mt: middle thoracic esophagus; Lt: lower thoracic esophagus; Ae: abdominal esophagus; SCC: squamous cell carcinoma; pT: pathological T stage; pN: pathological N stage.
*$P < 0.05$: Fisher's exact test.

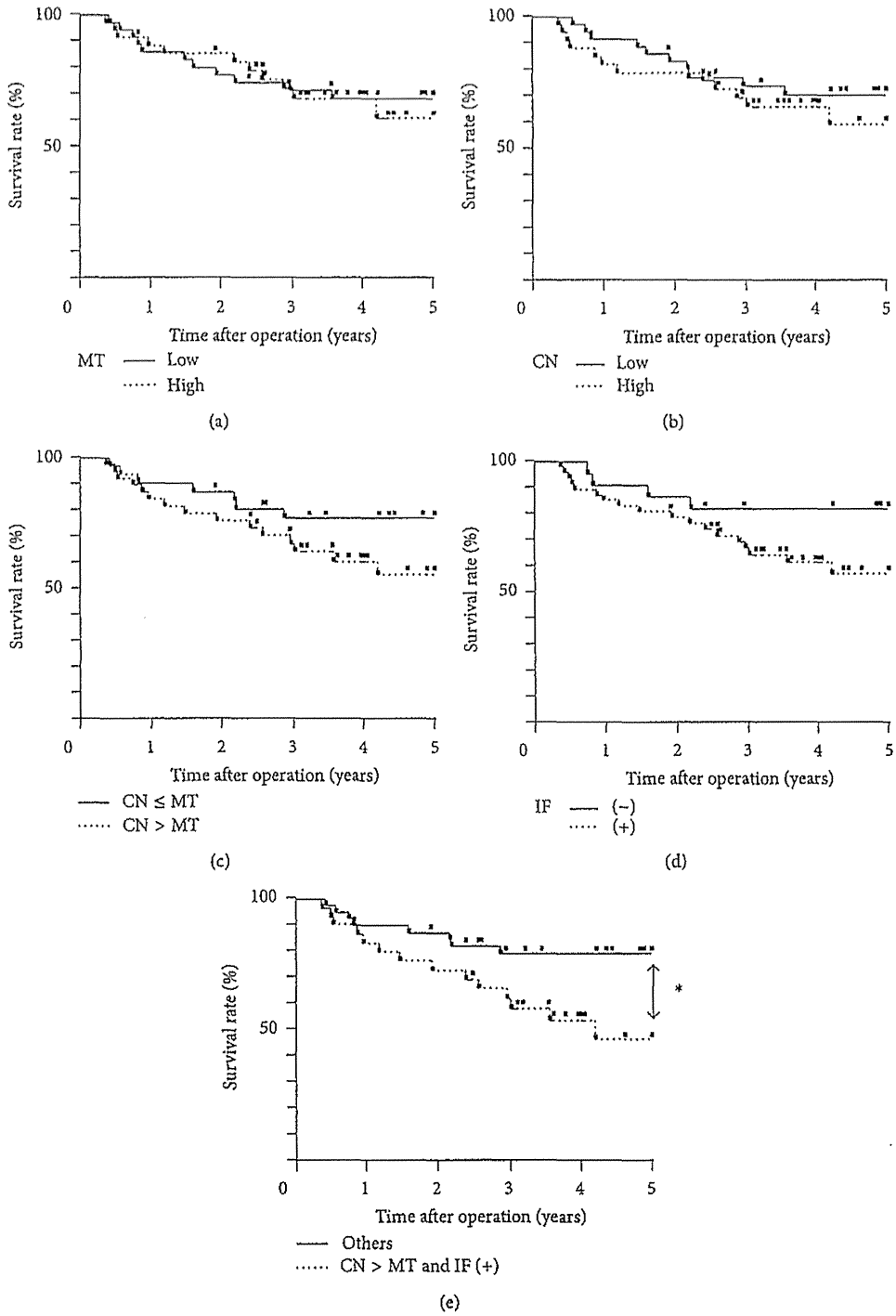


FIGURE 3: Survival curve of patients after curative resection for esophageal squamous cell carcinoma (ESCC) according to the expression of KCC3. (a) Patients were classified into two groups: low grade expression of KCC3 ($n = 35$) and high grade expression of KCC3 ($n = 35$) in the main tumor (MT). (b) Patients were classified into two groups: the low grade expression of KCC3 ($n = 36$) and high grade expression of KCC3 ($n = 34$) in the cancer nest (CN). (c) Patients were classified into two groups based on comparisons of the KCC3 score: CC ≤ MT ($n = 31$) and CN > MT ($n = 39$) in the cancer nest (CN). (d) Patients were classified into two groups based on the expression of KCC3 in the invasive front of the tumor: negative ($n = 22$) and positive ($n = 48$). (e) Patients were classified into two groups: patients with CN > MT and invasive front positive ($n = 31$) and others ($n = 39$). $^*P < 0.05$: log-rank test.